Supporting Information for:

Nitrite reduction mediated by heme models. Routes to NO and HNO ?

Julie L. Heinecke, Chosu Khin, Jose Clayston Melo Pereira, Sebastián A. Suárez, Alexei V. Iretskii, Fabio Doctorovich, and Peter C. Ford*

Table of Contents

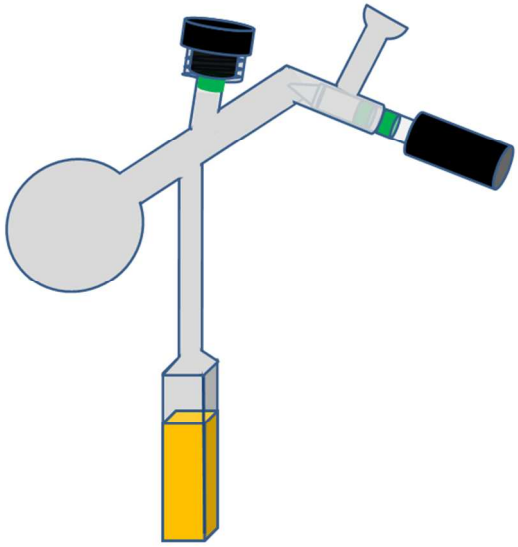

Figure S-1. Example of the specialized Schlenk-type cuvette used for the preparing anaerobic solutions on a vacuum line for the optical absorbance or photoluminescence spectroscopy and for kinetics measurements. The injection port on the top is used for additions of substrate needed to start reactions and for withdrawing gas samples for GC analysis. With a reaction solution volume (yellow) of 3.0 mL, the head-space of this cell was 28.0 mL

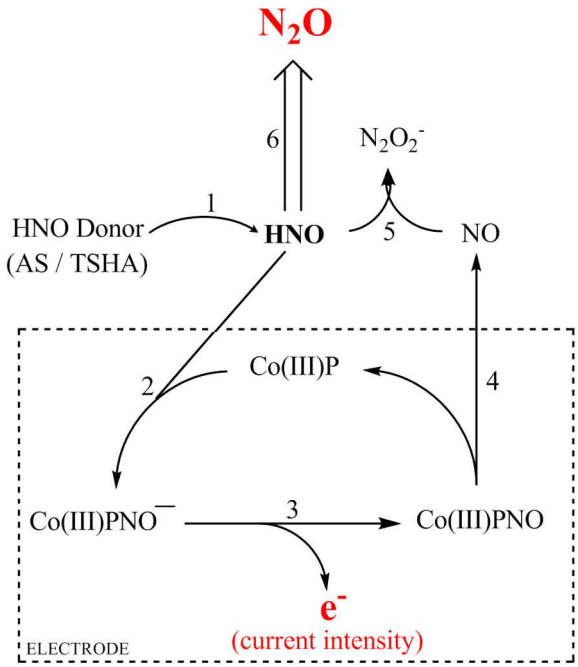

Scheme S-1. Mechanistic scheme considered for HNO production from the decomposition of AS, plus the reactions occurring at the electrode surface.

Table S-1. Reactions, rate laws, and rate constants that were used in the simulations for HNO production in the OAT reaction cycle (reactions numbered R1-R6 according to **Scheme S-1**).

	Reaction	Rate constant	ref
R1	Angeli's salt $\longrightarrow$ HNO	k_{dec} = 8.9 x 10^{-4} s^{-1}	1
R2	Co^{III}(Por) + HNO $\longrightarrow$ Co^{III}(Por)(NO^-) + H^+	k_{on} = 3.1 x 10^4 M^{-1} s^{-1}	2
R3	Co^{III}(Por)(NO^-) $\longrightarrow$ Co^{III}(Por)(NO) + e^-	k_{ox} = 0.089 s^{-1}	2
R4	Co^{III}(Por)(NO) $\longrightarrow$ Co^{III}(Por) + NO	k_{off} = 0.11 s^{-1}	2
R5	HNO + NO $\longrightarrow$ $N_2O_2^-$ + H^+	k_5 = 5.8 x 10^6 M^{-1} s^{-1}	3
R6	2 HNO $\longrightarrow$ N_2O + H_2O	k_{dim} = 8 x 10^6 M^{-1} s^{-1}	4

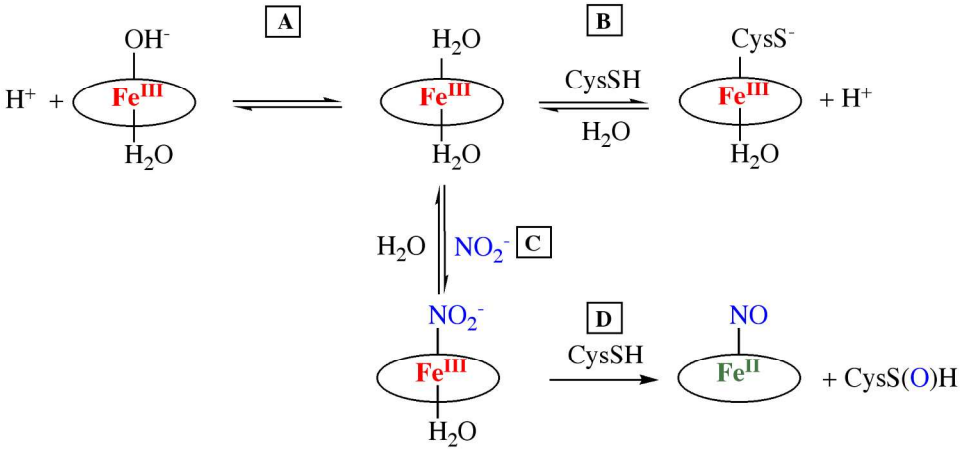

Scheme S-2. Illustration of the multiple reactions involving the ferric diaquo complex Fe^{III}(TMPS)$(H_2O)_2$ (**3**). Formation of the nitrosyl complex Fe^{III}(TMPS)(NO) (4) by OAT to CysSH (step D) occurs after reversible formation of Fe^{III}(TMPS)(NO_2^-) (C). The reaction is complicated by two "dead-end" equilibria, the formation of the monothiolate Fe^{III}(TMPS)($CysS^-$)(B) and formation of the monohydroxo complex Fe^{III}(TMPS)$(H_2O)(OH^-)$(A). (The pKa of **3** has been determined to be 6.9).[5]

[1] Miranda, K. M. *Coord. Chem. Rev.* **2005**, *249*, 433-455
[2] Suarez, S .A.; Fonticelli, M. H.; Rubert, A. A.; de la Llave, E.; Scherlis, D.; Salvarezza, R. C.; Martı´, M. A.; Doctorovich, F. A. *Inorg. Chem.* **2010**, *49*, 6955–6966.
[3] Lymar, S.V.; Shafirovich, V.; Poskrebyshev G.A.; *Inorg. Chem.* **2005**, *44*, 5212-5221.
[4] Shafirovich, V.; Lymar, S. V. *Proc. Natl. Acad. Sci. (USA)*, **2002,** *99,* 7340-7345.
[5] Wolak, M.; van Eldik, R. *J. Am. Chem. Soc*. **2005**, *127*, 13312–13315.

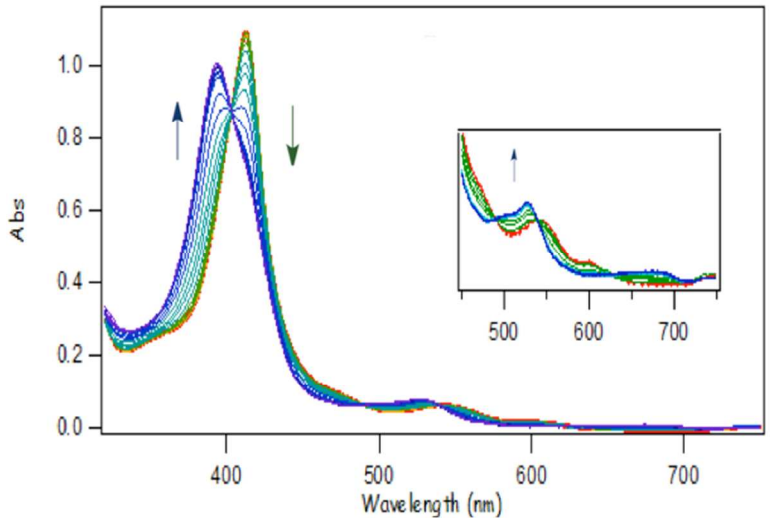

Figure S-2. Temporal spectral changes showing the reforming of Fe^{III}(TPPS) from a deaerated pH 5.81 solution containing Fe^{II}(TPPS)(NO) prepared by the reaction of **1** (7.4 x 10^{-6} M), tppts (6.6 x 10^{-4} M) and $NaNO_2$ (5.0 x 10^{-3} M) at 298 K observed over a period of 7 h.

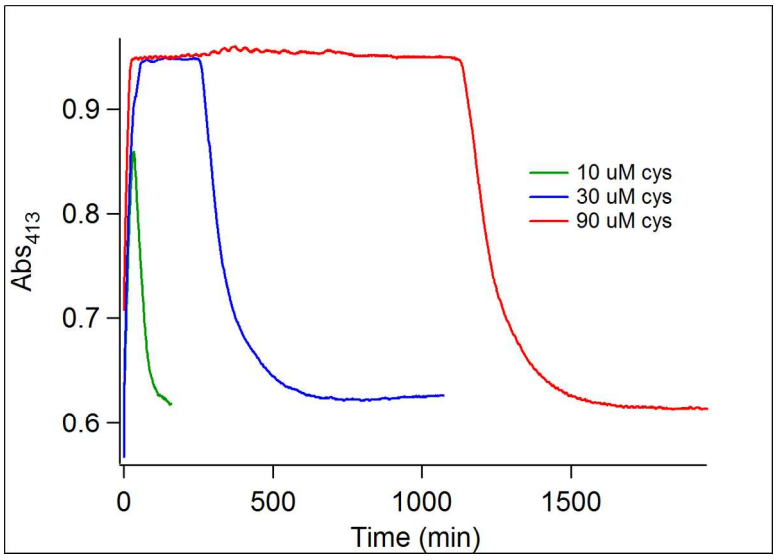

Figure S-3. The temporal absorbance changes at 413 nm for reaction of Fe^{III}(TPPS) (8.6 μM) and NO_2^- (10 mM) with varying concentrations of cysteine (10–90 μM) at pH 5.81 (50 mM phosphate buffer) at 25 ^oC. These show the fast formation of Fe^{II}(TPPS)(NO) (λ_{max} 413 nm) followed by a lag phase where that species is the principal chromophore in the solution, then eventual return to the initial spectrum of Fe^{III}(TPPS).

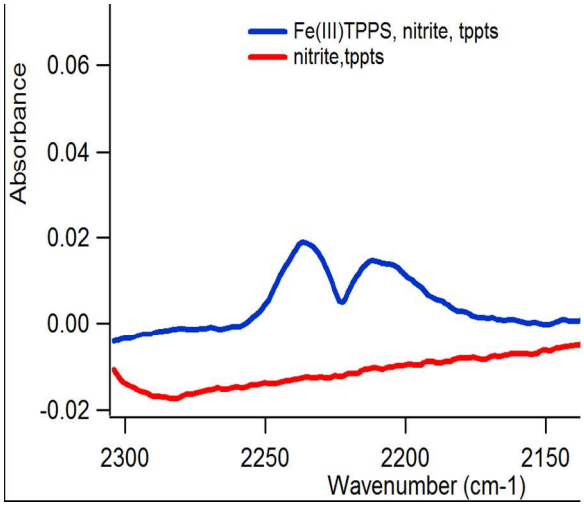

Figure S-4. Low resolution FTIR spectra of the headspace after the reaction of Fe^{III}(TPPS) (8.6 μM), $NaNO_2$ (10 mM) and tppts (1 mM) (blue) and of a control experiment containing only nitrite and tppts (red) (12 h reaction time). The former shows the characteristic P and R branches at 2211 cm^{-1} and 2235 cm^{-1} for the N_2O stretching vibrations.

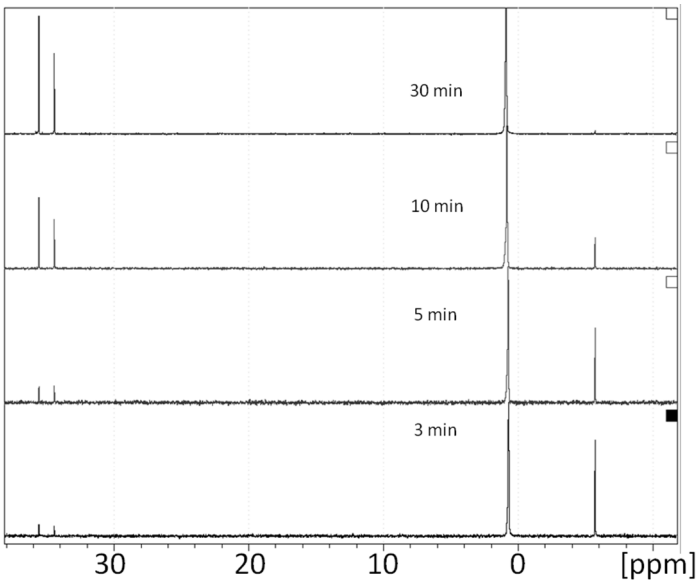

Figure S-5. Temporal dependence of the $^{31}P\{^1H\}$–NMR spectra for the reaction of Angeli's salt (HNO donor) (0.05 mmol) with tppts (0.05 mmol) in 0.6 mL at pH 5.81 solution (50 mM phosphate buffer, 10% D_2O). The loss of tppts (-5.0 ppm) is accompanied by ~1:1 formation of tpptsO (34.5 ppm) and tppts(NH) (35.5 ppm) over a period of 30 min..

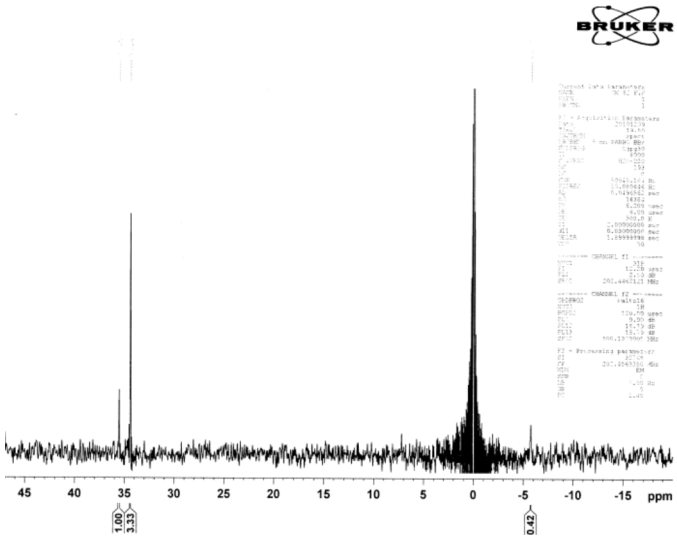

Figure S-6. The $^{31}P\{^{1}H\}$–NMR spectrum recorded for a pH 5.81 solution (50 mM phosphate) originally containing (Fe^{III}(TPPS) (8 μM), nitrite (10 mM) and tppts (1 mM). The spectrum shows that nearly all the tppts (-5.1 ppm) has been consumed and indicates formation of tpptO (34.5 ppm) and tppts(NH) (35.5 ppm).

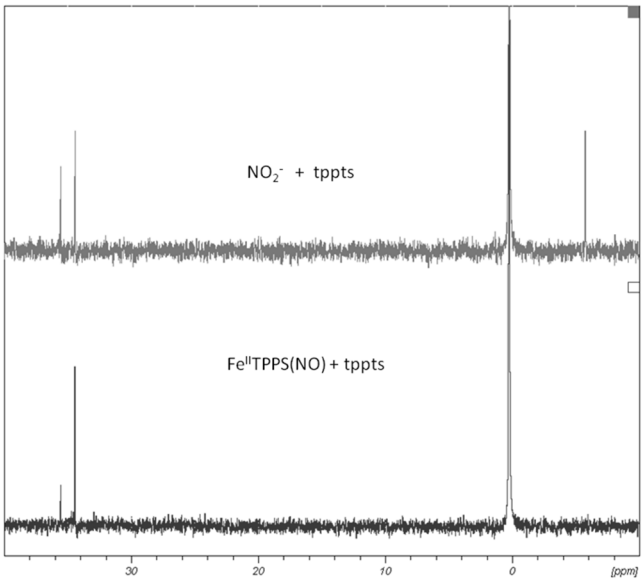

Figure S-7. *Top:* $^{31}P\{^{1}H\}$–NMR spectrum for the products of the reaction between nitrite (5 mM) and tppts (1 mM). *Bottom*: Spectrum for the products of the system composed of Fe^{II}(TPPS)(NO) (8 μM) nitrite (5 mM) and tppts (1 mM). Both are pH 5.81 (50 mM phosphate/10% D_2O) and the spectra of these two systems both indicate formation of tpptsO (34.5 ppm) and of tppts(NH) (35.5 ppm).

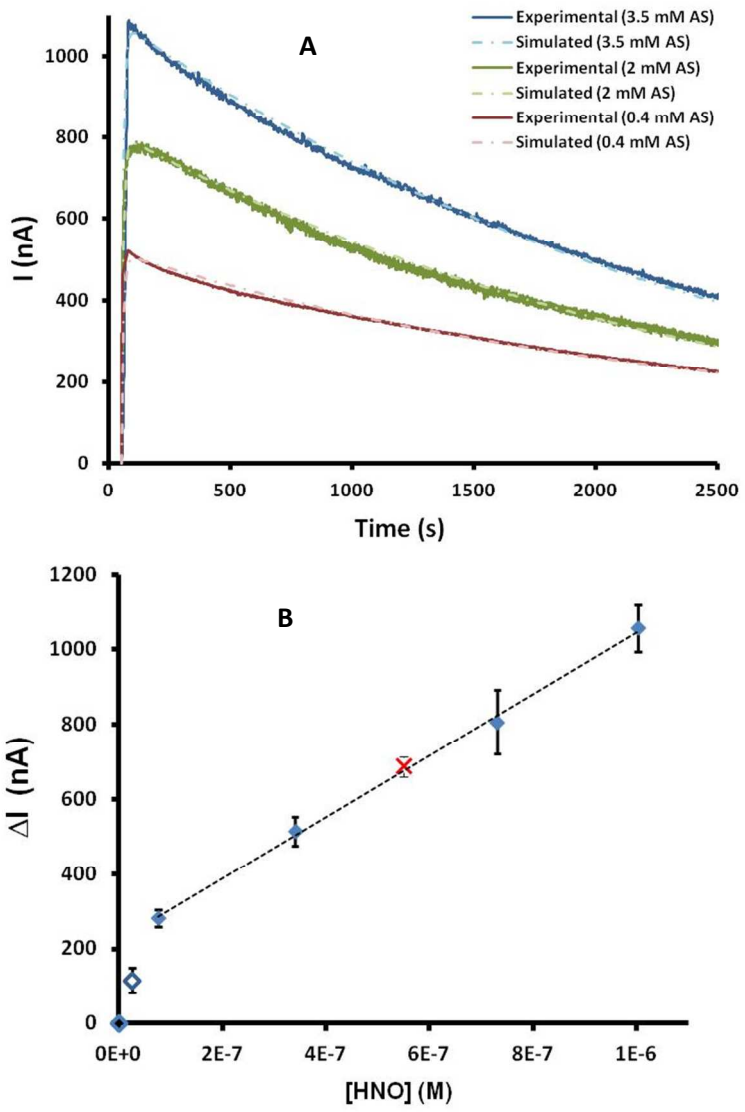

Figure S-8. A) Current intensity vs. time measured for three different concentrations of AS. In dotted lines are shown the corresponding simulations for the current intensity obtained from Co(III)PNO^{-} oxidation, by using the model shown in Scheme S-2. B) Calibration curve for the maximum [HNO] obtained from AS decomposition (as calculated in Scheme S-2) vs. measured current. Filled blue diamonds show the points used for the linear regression (2 or 3 independent measurements were done in each case); the red cross shows the maximum [HNO] generated by the reaction under study (for tppts 1.5 mM).

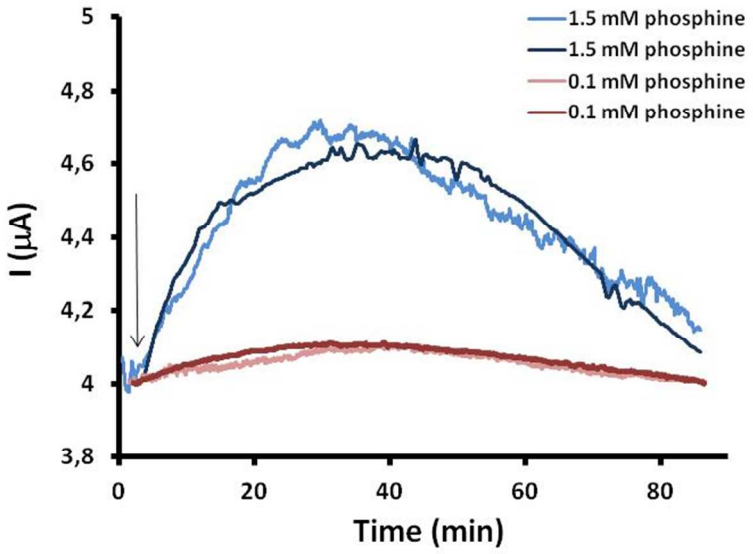

Figure S-9. Current detected using the cobalt modified gold electrode from pH 5.81 buffered solutions prepared from Fe^{III}(TPPS) (8 μM), sodium nitrite (10 mM) and tppts at 1.5 mM (blue) or 0.1 mM (pink). $NaNO_3$ 0.1 M was added as supporting electrolyte.

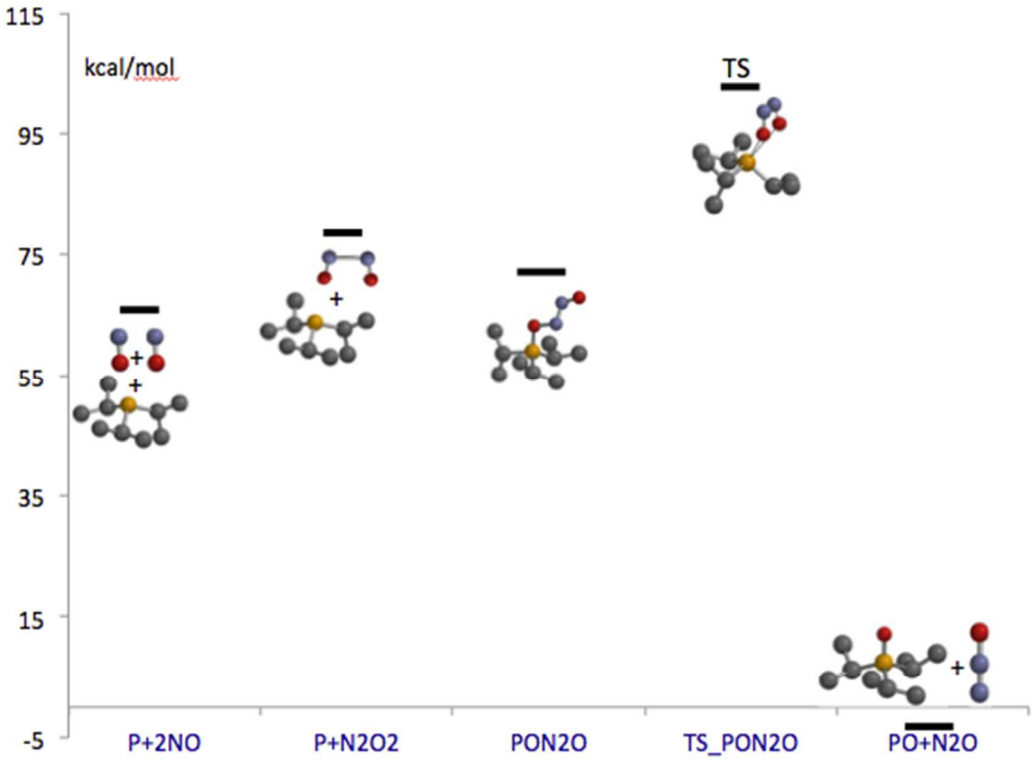

Figure S-10: DFT (B3LYP/6311+G**) computational results for the gas phase reaction of R_3P (R = ^{i}Pr) and NO.

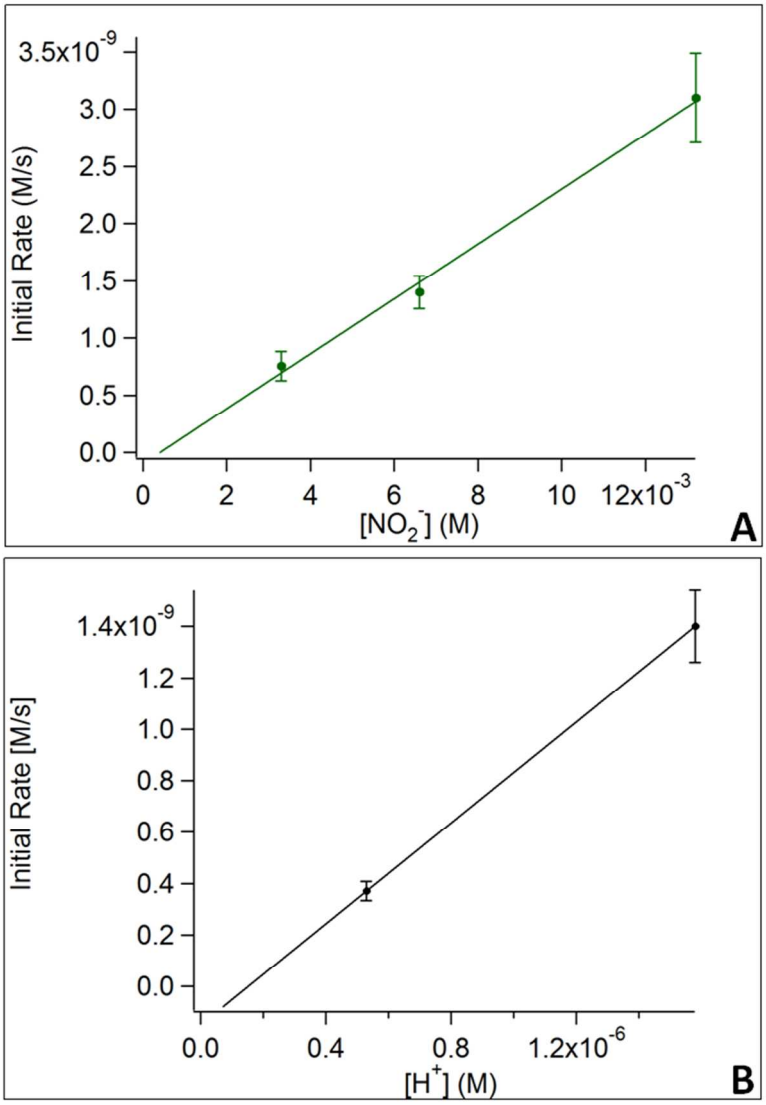

Figure S-11. Dependence of initial rate for nitrite reduction by Fe^{II}(TPPS) on $[NO_2^-]$ (A) and on $[H^+]$ (B).

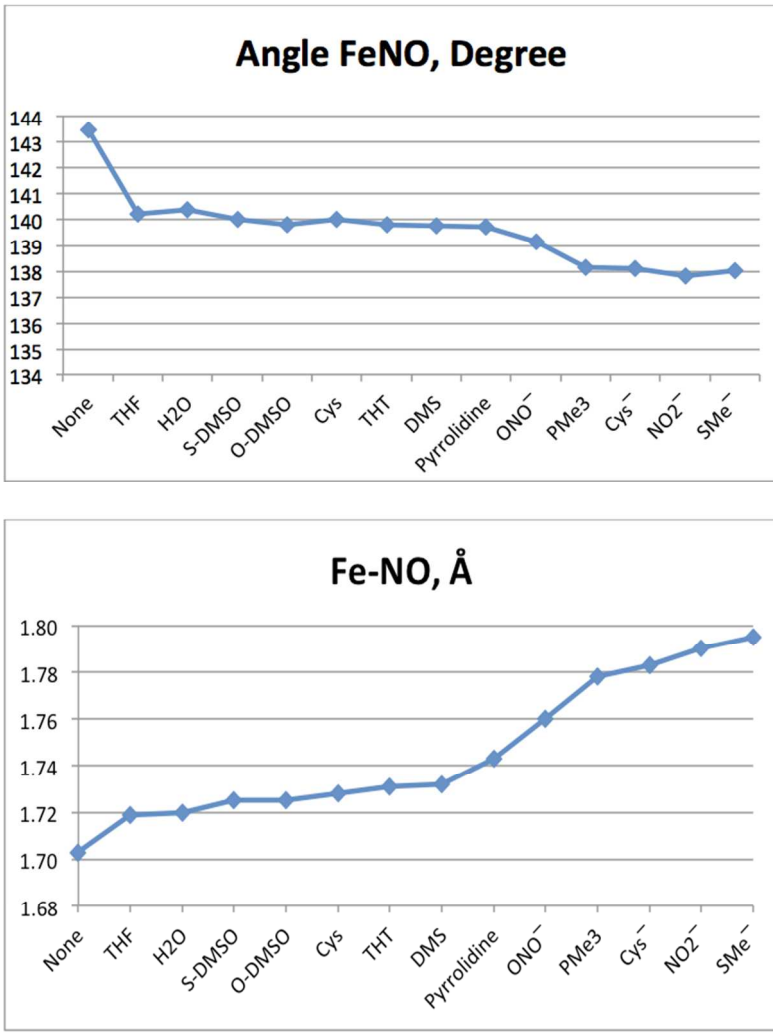

Figure S-12. DFT (unrestricted TPSSTPSS/DGDZTVP) computed Fe-N-O bond angles (top) and and Fe-NO bond lengths (bottom) for the complexes $Fe^{II}(P)(L)(NO)$, where P^{2-} is the porphinato dianion, and L is the proximal ligand tetrahydrofuran (THF), H_2O, *S*- and *O*- dimethylsulfoxide (DMSO), cysteine (Cys), tetrahydrothiophene (THT), dimethylsulfide (DMS), pyrrolidine, O-nitrito, trimethylphosphine (PMe3), Cysteinato (Cys–), N-nitrito or methylsulfido.